

Asymmetric bistable reflection and polarization switching in a magnetic nonlinear multilayer structure

Vladimir R. Tuz^{a,b,*}, Denis V. Novitsky^c, Sergey L. Prosvirnin^{a,b} and Sergei V. Zhukovsky^d

^a*Institute of Radio Astronomy of National Academy of Sciences of Ukraine, 4, Chervonopraporna St., Kharkiv 61002, Ukraine;* ^b*School of Radio Physics, V.N. Karazin Kharkiv National University, 4, Svobody Sq., Kharkiv 61022, Ukraine;* ^c*B.I. Stepanov Institute of Physics of National Academy of Sciences of Belarus, 68, Nezavisimosti Avenue, Minsk 220072, Belarus;* ^d*DTU Fotonik – Department of Photonics Engineering, Technical University of Denmark, Ørstedes Pl. 343, DK-2800 Kgs.Lyngby, Denmark*

(v3.4 released October 2010)

Optical properties of a one-dimensional photonic structure consisting of Kerr-type nonlinear and magnetic layers under the action of an external static magnetic field in the Faraday geometry are investigated. The structure is a periodic arrangement of alternating nonlinear and magnetic layers (a one-dimensional photonic crystal) with one of the layers doubled to create a defect where periodicity is violated. Strong enhancement of nonreciprocity is observed at the frequencies of the defect modes, where linearly polarized light incident from one side of the structure undergoes 90° polarization rotation upon reflection, while light reflected from the other side has its polarization unchanged. Using the nonlinear transfer matrix calculations in the frequency domain, it is demonstrated that defect resonances in the nonlinear reflection spectra undergo bending, resulting in polarization bistability of reflected light. This bistability is shown to result in abrupt switching between linear polarization of the output reflected light when the input intensity is varied. This switching is confirmed in finite-difference time-domain simulations, and its hysteresis character is established.

Keywords: magnetophotonic crystal; bistability; nonreciprocity

1. Introduction

In classical electromagnetism, the reciprocity theorem is based on the Lorentz lemma [1]. It states that the relationship between an oscillating current and the resulting electric field is unchanged if one interchanges the points where the current is placed and where the field is measured; this statement is also called Helmholtz reversion-reciprocity principle [2]. In the proof of the reciprocity theorem it is assumed that the medium where the field propagates is linear and isotropic. For anisotropic media, the reciprocity theorem holds only in the case when the tensors of material parameters of the medium are symmetric. Otherwise, such as in the case of gyrotropic media (for example, in magnetic materials), the asymmetry in the tensor of permittivity or permeability makes the reciprocity theorem no longer valid.

Nonreciprocity effects are known to be especially pronounced when magnetic materials are arranged to form strongly dispersive environments such as photonic crystals, rather than as bulk materials. In such environments, nonreciprocity is manifest as spectral asymmetry of dispersion curves $\omega(\vec{k}) \neq \omega(-\vec{k})$, and particularly arises in magnetophotonic crystals under the

*Corresponding author. Email: tvr@rian.kharkov.ua

action of an external static magnetic field in the Faraday geometry. It was found that in such magnetophotonic crystals [3, 4] and multilayer systems with structural gyrotropic layers (featuring light diffraction on a periodic structure of the medium [5, 6]) a substantial nonreciprocity enhancement is reached at the edges of the photonic band gaps. However, an even stronger localization of the field within the system and, accordingly, an even more significant nonreciprocity enhancement can be obtained by purposefully creating one or more defects (resonant cavities) in a periodic magnetophotonic structure. Using this technique, it is possible to obtain large values of nonreciprocity with relatively small values of the external magnetic field, which facilitates the use of such structures as optical isolators or one-sided optical reflectors.

On the other hand, the reciprocity theorem also does not hold for nonlinear media due to the role of dynamic effects [1]. Therefore, there is an apparent possibility to obtain new nonreciprocal effects in spatially inhomogeneous nonlinear media, including ones with dissipative losses. In such systems, a number of new nonreciprocal phenomena are revealed, among which spectral nonreciprocity, nonreciprocal compression [7], and nonreciprocal dynamics of self-induced transparency solitons [8] can be mentioned.

As is the case with magnetophotonic crystals, the nonlinearity-induced nonreciprocal response is also expected to be strongly enhanced in photonic structures comprising an asymmetrically located defect, or cavity, made of a nonlinear (e.g., a Kerr-type) dielectric. This enhancement occurs due to the strong field localization within the defect layer, which becomes different for the waves incident on the system from the opposite sides. Such *spatial-inversion asymmetry* results in a different coupling strength between the external field and the fields inside the cavity. This enhancement of nonreciprocal optical response, sometimes denoted as “reversible nonreciprocity” [9], can be the basis for designing, for example, optical diodes.

Note that reversible nonreciprocity in an asymmetric nonlinear photonic structure is usually accompanied by optical bistability (or, generally, multistability). This is a general property of any nonlinear system with feedback, meaning that two or more stable output states may exist for the same input state of the system. Such bistability can be seen in magnitude [10, 11] or polarization [12, 13] of the transmitted and reflected fields. The relation between input and output parameters of the system typically forms a hysteresis loop with singularities, where abrupt switching between the stable states occurs. One can make use of such switching to design active (rather than passive) optical diodes, isolators, and other polarization-control devices.

It is therefore insightful to investigate the effects of the *interplay* between the Faraday and the Kerr effects in the formation of optical nonreciprocity in a photonic structure setting, as well as the influence of such interplay on the dynamics of the bistable switching. A straightforward way to do so would be to combine a Faraday-active and a Kerr-nonlinear material in the same one-dimensional photonic structure with an asymmetrically placed defect. In this paper, we investigate spectral, polarization, and dynamic optical properties of such spatially asymmetric multilayers containing both magneto-optic and nonlinear materials.

By carrying out both frequency-domain (nonlinear transfer matrix) and time-domain (finite-difference time-domain) calculations, we show that combining magneto-optic and nonlinear materials in the same photonic multilayer structure results in many peculiar spectral and polarization properties. Using a periodic structure with an asymmetrically placed periodicity violation (a cavity or defect layer), we show that the nonreciprocal effect can be greatly enhanced by the interplay between the Faraday effect and the spatial-inversion asymmetry, leading to a very strong asymmetry in the polarization conversion via the defect modes even in the linear regime. Namely, a structure with a good coupling between the field in the defect and the incident field shows near-90° polarization rotation at the defect resonance frequencies, while the mirror-image structure (or the same structure when the direction of incident light is reversed) has poor coupling between the field in the defect and the incident field, causing polarization conversion effects to nearly vanish.

In the nonlinear regime, the bending of resonances in the nonlinear reflection spectra is shown

to lead to strong bistability between linearly polarized states, again exhibiting strong asymmetry with respect to the direction of light incidence. This bistability is shown to give rise to asymmetric polarization switching. Such switching, along with hysteresis loops in the multilayer input/output characteristics, is confirmed in time-domain numerical simulations.

The remainder of this paper is organized as follows. In Section 2, we describe in detail the geometrical and material parameters of the magnetic nonlinear multilayer structure under study, and outline the nonlinear transfer matrix method that was used to obtain the spectral properties of the structure. Section 3 follows with the results on these spectral properties in the linear and nonlinear regime. Strong polarization conversion, both input/output and polarization bistability properties are demonstrated. In Section 4, we present the numerical simulations results showing bistable switching between linear polarization states in the time domain. Finally, Section 5 summarizes the paper.

2. Problem formulation

2.1. Magnetophotonic nonlinear multilayers under study

We consider a planar multilayer stack of infinite transverse extent (Fig. 1). Each unit cell is composed of a bilayer which consists of magnetic layers Ψ (with constitutive parameters $\varepsilon_1, \hat{\mu}_1$) and nonmagnetic layers Υ (with parameters ε_2, μ_2). The magnetic layers Ψ are magnetized up to saturation by an external static magnetic field \vec{M}_0 directed along the z -axis (the Faraday geometry). We assume that each layer Υ is a Kerr-type nonlinear dielectric, which permittivity ε_2 linearly depends on the intensity $|E|^2$ of the electric field ($\varepsilon_2 = \bar{\varepsilon}_2 + \bar{\varepsilon}_2|E|^2$). A periodicity violation (defect) is created by joining two sections together in which the layers are alternating in the different order. So, the defect (repeating two layers of the same type) can be placed either symmetrically or asymmetrically in the structure. The parameters m and n denote the number of bilayers placed before and after the periodicity violation. In any case the bilayers are arranged symmetrically with respect to the defect, i.e. the structure begins and ends with layers of the same type. We suppose that all layers have the same thickness D . The outer half-spaces $z \leq 0$ and $z \geq \Lambda$ ($\Lambda = 2(m+n)D$) are homogeneous, isotropic, and have material parameters ε_0, μ_0 .

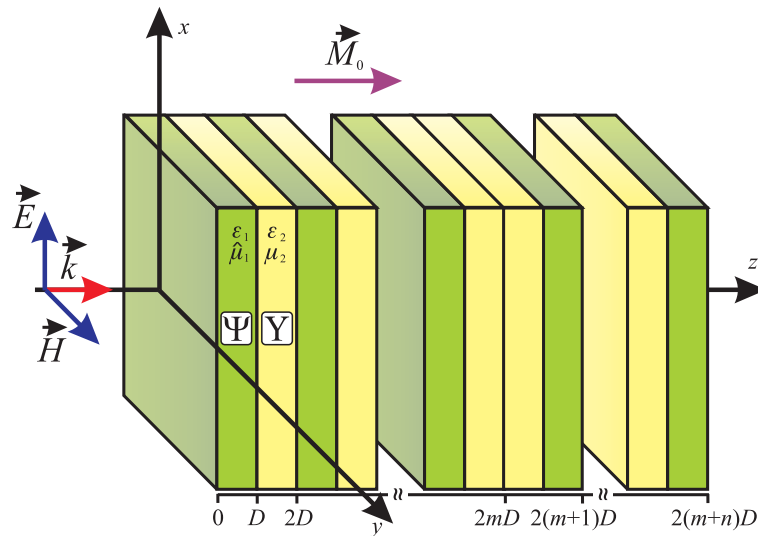


Figure 1. (Color online) Periodic photonic multilayer with a defect containing nonlinear and magnetic layers in the Faraday geometry.

Let us assume that the normally incident field is a linearly polarized plane monochromatic

wave of a frequency ω and an amplitude A . For the sake of definiteness, we also suppose that the vector \vec{E} of the incident wave is directed along the x -axis.

A nomenclature of materials which can be used to construct the proposed structure was previously discussed in [13]. It was based on the book [14] and reviews on magnetophotonic crystals [3, 4]. So we suppose that magnetic layers Ψ can be made from impurity-doped yttrium-iron garnet (YIG) films, since they are transparent in the near infrared region. As a material for nonlinear layers Υ , either GaAs or InSb can be selected. Based on [15], we expect that nonlinear response of the proposed structure becomes apparent at the input light intensity about 1-10 kW/cm².

In the Faraday geometry when the external static magnetic bias is parallel to the wave propagation direction ($\vec{k} \parallel \vec{M}_0$), the magnetic permeability $\hat{\mu}_1$ is a tensor with off-diagonal components:

$$\hat{\mu}_1 = \begin{pmatrix} \mu_1^T & i\alpha & 0 \\ -i\alpha & \mu_1^T & 0 \\ 0 & 0 & \mu_1^L \end{pmatrix}. \quad (1)$$

Throughout the paper the working frequencies are supposed to be far from the frequency of the ferromagnetic resonance of magnetic layers and band edge of semiconductors such as GaAs are used as nonlinear materials, so we will assume that losses in the whole structure are negligibly small. Also, in the chosen frequency band the diagonal components (μ_1^T, μ_1^L) of the magnetic permeability (1) are close to unity while the off-diagonal ones ($\pm i\alpha$) are small but non-zero.

2.2. Nonlinear transfer matrix method

In the studied structure configuration, in the frequency domain, our solution is based on the 4×4 -transfer matrix formulation [16] which is used to calculate the inner field distribution and the reflection and transmission coefficients of the system. However, this field structure influences the permittivity of the nonlinear layers through the Kerr effect. Therefore, spectral and polarization properties of the multilayers under study are determined using some nonlinear modification of the transfer matrix method.

Thus, in the *linear regime*, the equation that defines the coupling of the tangential field components at the input and output of the magnetophotonic structure is written as [12, 13]

$$\vec{V}(0) = \mathfrak{M}\vec{V}(\Lambda) = \{(\Psi\Upsilon)^m(\Upsilon\Psi)^n\} \vec{V}(\Lambda), \quad (2)$$

where $\vec{V} = \{E_x, E_y, H_x, H_y\}^T$ is the vector containing the tangential field components at the structure input and output, the upper index T denotes the matrix transpose operation, Λ is the total length of the structure; Ψ and Υ are the transfer matrices of the rank four of the magnetic and nonmagnetic layers, respectively. The elements of the transfer matrices in Eq. (2) are determined from the solution of the Cauchy problem and are presented in [16].

Once the solution of the linear problem (2) is evaluated, the intensity of the reflected and transmitted fields and the distribution of the field $\vec{E}_{in}(z)$ inside the system are calculated. When the structure consists of a Kerr-type nonlinear layers (in the *nonlinear regime*), the permittivity ε_2 depends on the intensity of the electric field within each layer Υ as follows

$$\varepsilon_2(z) = \bar{\varepsilon}_2 + \bar{\varepsilon}_2 |E_{in}(z)|^2. \quad (3)$$

Nevertheless, the nonlinearity becomes only apparent within the defect layers, because here the field is localized most strongly. Since the thickness of the defect is comparable to the wavelength in the medium, and hence the intensity variation across the defect thickness needs to be taken

into account, we break up both Υ -layers within the defect into a number of thin sublayers Υ_j with thicknesses $d_j \ll \lambda$ which are described with corresponding matrices Υ_j :

$$\vec{V}(0) = \mathfrak{M}\vec{V}(\Lambda) = \{(\Psi\Upsilon)^{m-1}\Psi(\Upsilon_1 \dots \Upsilon_L)\Psi(\Upsilon\Psi)^{n-1}\} \vec{V}(\Lambda). \quad (4)$$

We can then consider the dependence of ε_2 on the average intensity of the electric field $|\overline{E_{in}}|^2$ inside each such sublayer. Knowing the field intensity in each sublayer Υ_j , the actual value of transfer-matrix \mathfrak{M} of the whole structure can be calculated. Thus we deal with a system of nonlinear equations on the unknown function of the field intensity distribution inside the sublayers Υ_j . A magnitude of the incident field A appears as an independent parameter of this equations set. This system of nonlinear equations related to the average field intensity distribution in the sublayers is solved numerically. The solution yields us the final field distribution in the photonic structure and the values of the reflection R and transmission T coefficients; the reader is referred to Ref. [16] for further details.

3. Spectral properties and polarization bistability

In linear optics it is well known that a magnetophotonic structure in the Faraday configuration has circularly polarized eigenstates and exhibits dichroism, which leads to the tendency for arbitrary polarized waves to acquire a polarization state of one of the eigenwaves of the system as the incoming light propagates through it [16]. In the general case, the result is that the waves become elliptically polarized after reflection from and transmission through the magnetophotonic structure. A very important point is that the spectral dependence of the output polarization state does not have any discontinuities, and the degree of polarization transformation depends only on the static magnetic field strength.

However, as we mentioned in the Introduction, the situation is very different in the nonlinear optical regime. The dependence of material parameters on the intensity of light can lead to polarization bistability, multistability [12, 13, 17, 18] or even to polarization chaos [19]. These effects manifest themselves in such a way that the output wave polarization state becomes a multivalued function, containing both stable and unstable branches.

This multivalued character brings about several important consequences. First, hysteresis loops are known to appear in the system, both in its input-output characteristic and in its nonlinear transmission and reflection spectra [20]. Second, the frequency dependence of the Stokes parameters for the reflected and transmitted waves shows discontinuous behavior. Third, the output polarization states may depend on the history of the system, determined by its temporal evolution. In order to adequately demonstrate the nonlinear features of the studied structure, both frequency-domain and time-domain calculations are this warranted.

In this Section, we begin by analyzing the transmission and reflection spectra of the magnetic nonlinear structure under study. Since the whole system possesses axial symmetry in the considered case of normal incidence and Faraday geometry, we will only distinguish between copolarized (e.g. *ss* or *pp*, denoted *co*) and cross-polarized (*sp* or *ps*, denoted *cr*) components throughout the calculations.

3.1. Linear spectral properties

In the linear regime the basic optical features of the studied structure are determined by both the property of its periodicity and the presence of magnetic layers. As a result of the structure periodicity, the spectra have interleaved bands with high and low level of reflection (stopbands and passbands) which are typical for all photonic structures when the thickness of their layers

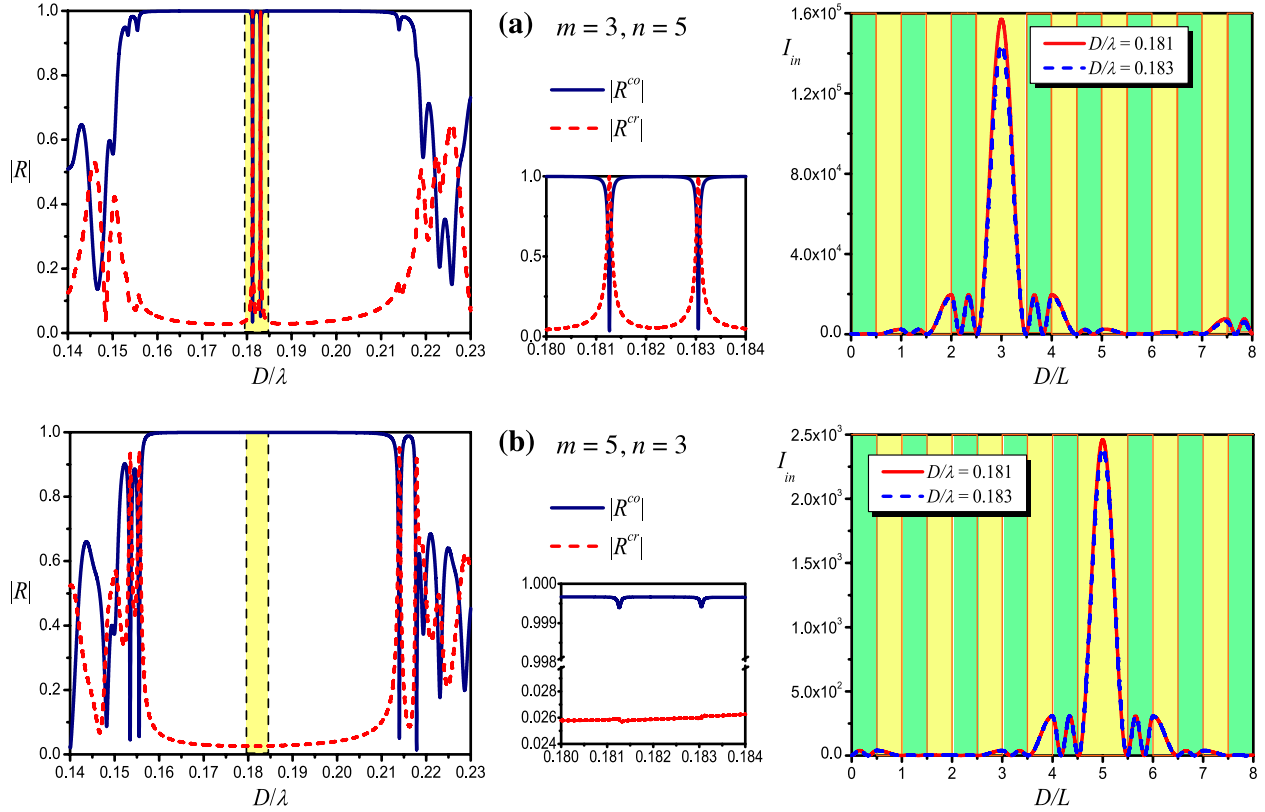


Figure 2. (Color online) Reflection spectra (*left*) and field intensity distributions (*right*) for the magnetophotonic structure with asymmetrically placed defect in the linear regime for (a) $m = 3, n = 5$ and (b) $m = 5, n = 3$. The spectra show the magnitudes of the copolarized (co) and cross-polarized (cr) components of the reflection coefficients for linearly polarized waves. The insets (*middle*) show an enlarged view of the region of interest (D/λ from 0.18 to 0.184). Note the difference in the intensity scale by two orders of magnitude between the field distribution plots for (a) and (b). The parameters of the structures are $\varepsilon_1 = 16$, $\varepsilon_2 = 2$, $\mu_1^T = \mu_1^L = \mu_2 = 1$, $\alpha = 0.02$.

is comparable to the wavelength. The corresponding fragment of the reflection spectra where there is a stopband is presented in Fig. 2. If any periodicity violation (a “defect”) is introduced inside the system, some resonances can appear in the stopbands, with the field strongly localized inside the defect. The existence of such localized resonances is explained by the fact that the periodicity violation forms a resonant Fabry-Perot cavity enclosed between two Bragg mirrors.

Since the structure consists of magnetic layers under the action of the external static magnetic field in the Faraday configuration, and thus its eigenwaves are left-circular-polarized (LCP) and right-circular-polarized (RCP) waves propagating inside the system with different speeds [16]. Thus the structure reacts differently to circularly polarized waves with opposite handedness, which results in distinct resonant conditions for the LCP and RCP waves. Since the incident linearly polarized wave is a superposition of two equal-amplitude circularly polarized components of opposite handedness and different phase, induced by the external static magnetic field, the localized resonances in stopbands split into doublets where the position of each peak on the frequency scale is defined by the corresponding resonant frequency of the RCP and LCP waves. At the same time, the distribution of the intensity of the field inside the structure is almost identical on both the resonant frequencies (Fig. 2).

It is obvious that if the Bragg mirrors on each side of the cavity layer have a different number of layers, the properties of the structure become different for the waves incident on the structure from the left and right. First of all this difference is manifest in the intensity magnitude of the field localized inside the defect, which can be seen in Fig. 2. From a mathematical point of view, this property follows from the noncommutativity of the transfer-matrices product in Eq. (2).

This intensity difference strongly affects on the formation of localized resonances in the stop-

bands. When the configuration of the Bragg mirrors is chosen in such a way that the first mirror has lower reflectivity ($m = 3$) while the second one has higher reflectivity ($n = 5$), the field localization profile inside the defect is very strong, forming two clearly defined resonances at D/λ between 0.18 and 0.184, where strong polarization conversion is seen to occur. In the reverse configuration, ($m = 5$, $n = 3$), where the highly reflective mirror is between the incident wave and the defect, the field localization pattern looks quite similar but the localized field intensity is about 100 times smaller, and the resonances in the stopband become extremely weakly pronounced, as seen in the inset of Fig. 2 (b).

It should be pointed out that this strong asymmetry is the result of an interplay between the geometrical asymmetry of the structure and the nonreciprocity caused by the Faraday effect. Indeed, in the absence of magnetic fields the reciprocity theorem would require that the field localization pattern be similar for both configurations, and that transmission and reflection peaks corresponding to a defect resonance be of similar height [21] for two mirror-symmetric configurations. However, the Faraday effect violates this condition, which enhances resonances where there is a good coupling between the incident wave and the defect ($m = 3$, $n = 5$).

In one-dimensional photonic crystals, the field intensity concentrated in the defect layer is known to reach its maximum when the refractive index of this layer is less than the refractive index of the remaining structure [22]. Providing this condition by a proper choice of geometrical and material parameters of the multilayer, total cross-polarization transformation in the reflected field can be reached at the defect resonances. Thus, the near-total linear polarization conversion

$$|R^{co}| = 0 \text{ and } |R^{cr}| \approx 1, \quad (5)$$

can be achieved in the ($m = 3$, $n = 5$) configuration. This can be seen in the insets of Fig. 2 (*middle column*) where the resonance region is highlighted. Conversely, the other configuration ($m = 5$, $n = 3$) with poorer coupling between the defect and the incident wave experiences the reverse effect: the field localization is weakened and polarization conversion is largely suppressed.

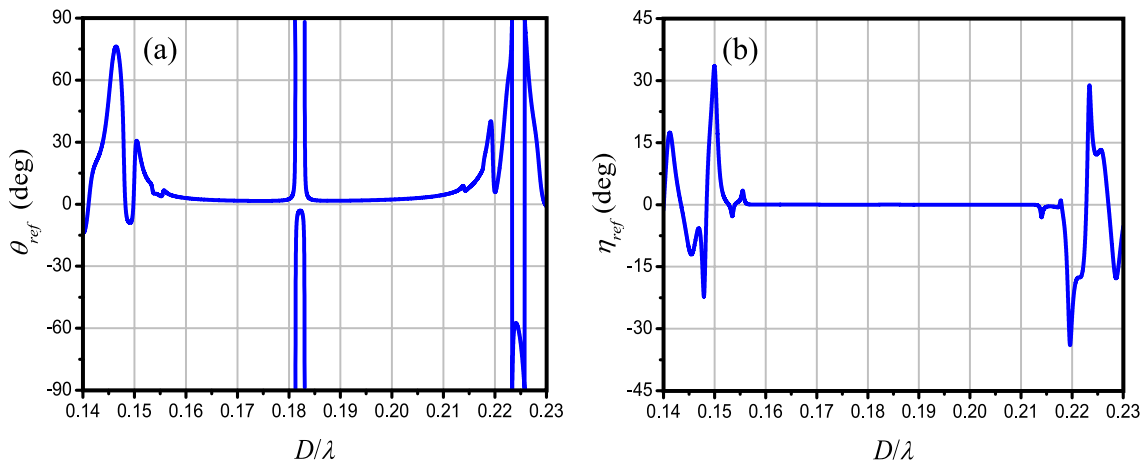


Figure 3. (Color online) Frequency dependences of (a) the polarization azimuth θ and (b) the ellipticity angle η of the reflected field in the linear regime. The incident light is linearly polarized, and structure parameters are as in Fig. 2.

Furthermore, the time-reversal asymmetry of the magnetic layers leads to a change of the polarization state of the reflected field. This polarization change is confirmed in Fig. 3, which shows the corresponding frequency dependences of the polarization azimuth (θ) and the ellipticity angle (η) for the reflected field. According to the definition of the Stokes parameters, we introduce the ellipticity η so that the field is linearly polarized when $\eta = 0$. The case $\eta = -\pi/4$ (-45°) corresponds to LCP, and the case $+\pi/4$ ($+45^\circ$) corresponds to RCP. In all other cases ($0 < |\eta| < \pi/4$), the field is elliptically polarized. In the considered frequency band and in the linear

regime, the reflected field is seen to be linearly polarized throughout the whole stopband [Fig. 3 (b)], and it acquires a rotation of the polarization plane on 90° exactly at the frequencies of the localized resonances. This is in full accordance with Fig. 2 (a).

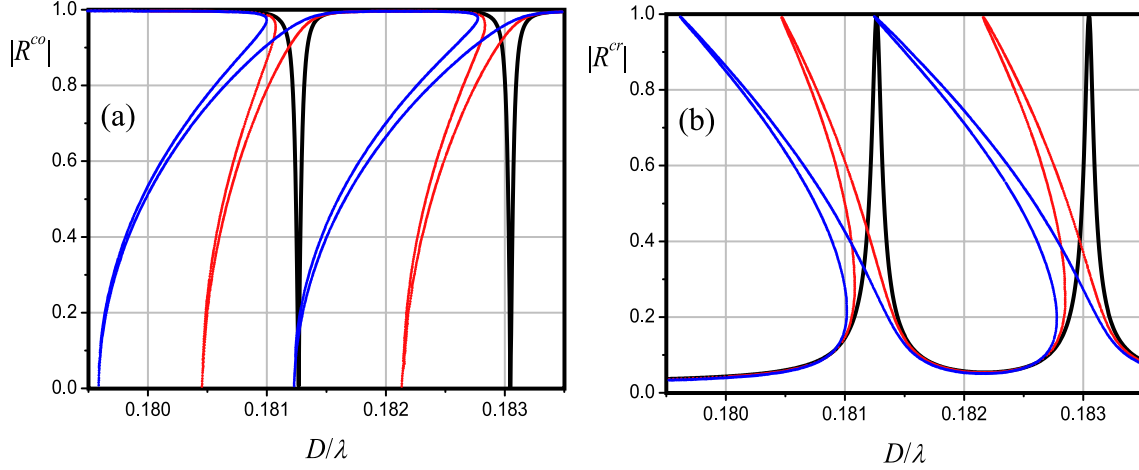


Figure 4. (Color online) Frequency dependences of the magnitudes of (a) the copolarized (co) and (b) cross-polarized (cr) components of the reflection coefficients of linearly polarized waves. In the nonlinear regime the input intensity I_0 is taken to be 5 and 10 kW/cm^2 . Other parameters are as in Fig. 2.

3.2. Nonlinear spectral properties

In the nonlinear regime the strong field localization in the defect changes the refractive index of the material within it. In our case $\bar{\epsilon}_2 > 0$, so, in the spectral characteristics it is known to result in bending of both localized resonance in the stopband towards lower frequencies [20] (Fig. 4). Therefore the reflection coefficient magnitude becomes a multivalued function. The degree of this resonance bending clearly depends on the intensity of the incident field and is nearly the same for both resonances in the doublet. Due to the above-mentioned polarization sensitivity in the system, a linearly polarized wave will undergo a change in its polarization state during the reflection also in the nonlinear regime. However, the conditions of Eq. (5) can still be met.

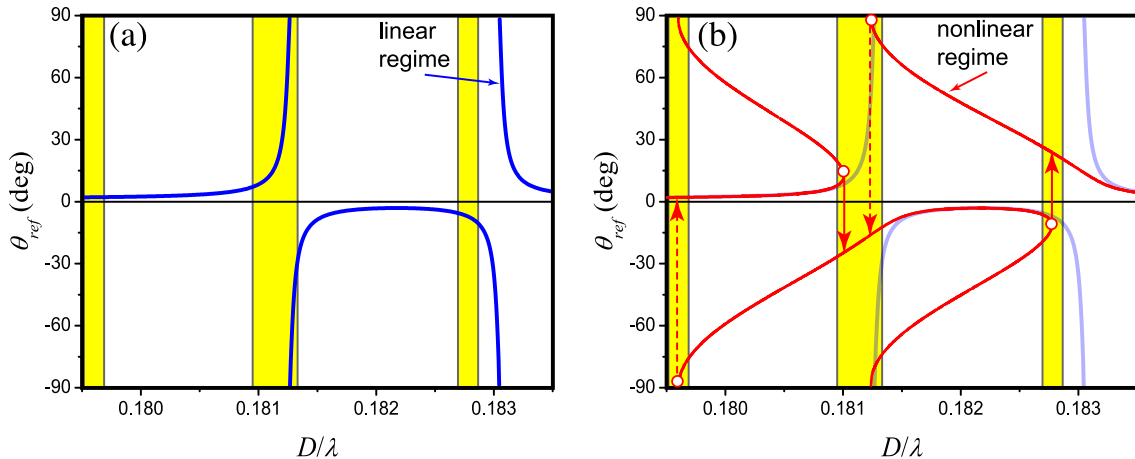


Figure 5. (Color online) Frequency dependences of the polarization azimuth θ_{ref} of the reflected field in the (a) linear and (b) nonlinear regime. In the latter the input intensity I_0 is taken to be 10 kW/cm^2 . Other parameters are as in Fig. 2.

Expectedly, the angle of rotation of the polarization ellipse (θ) in the nonlinear regime becomes a multi-valued function too (Fig. 5). However, the ellipticity angle η is found to remain

unchanged ($\eta = 0$). The ambiguity of θ and the associated bistability can be used to realize switching between two different polarization states in the reflected light. The frequency bands where this polarization instability takes place are marked in Fig. 5 as shaded areas. Switching between different polarization states occurs as hopping between the two stable branches when the frequency is varied. Such events are shown in Fig. 5 by solid and dashed arrows for increasing and decreasing frequency, respectively.

4. Time-domain simulation and polarization switching

The existence of bistability is a necessary but by no means a sufficient condition for practical realization of bistable switching, since the conditions needed to excite a particular branch of the hysteresis loop remain to be determined [10, 11]. Moreover, a hysteresis in the frequency is of limited use because a continuous sweep of the frequency would often be impractical in communication applications. Therefore, in this section we demonstrate bistable polarization switching in a magnetic nonlinear multilayer using time-domain simulations.

To study signal evolution in the considered structure, we start with a pair of wave equations for circularly-polarized electric fields $E_{\pm} = E_x \pm iE_y$ in the form

$$\frac{\partial^2 E_{\pm}}{\partial z^2} = \frac{\mu^{\pm}(z)}{c^2} \frac{\partial^2 D_{\pm}}{\partial t^2}. \quad (6)$$

Here $\mu^{\pm} = \mu_1^T \pm \alpha$ and $\mu^{\pm} = \mu_2$ in magnetic and dielectric layers, respectively, $D_{\pm} = \varepsilon(z)E_{\pm}$ is the electric displacement, the dielectric permittivity $\varepsilon(z, I) = n(z, I)^2$ containing spatial periodic modulation and nonlinear dependence on light intensity. The change of permittivity in the each nonlinear layer Υ is described by Eq. (3).

We solve Eqs. (6) numerically using the finite-difference time-domain (FDTD) method similar to that one developed in Ref. [23]. For convenience, we represent field strengths as $E_+ = A(t, z) \exp[i(\omega t - kz)]$ and $E_- = B(t, z) \exp[i(\omega t - kz)]$, where ω is a carrier frequency, $k = \omega/c$ is the wavenumber, and then solve equations for the amplitudes $A(t, z)$ and $B(t, z)$. Finally, introducing dimensionless arguments $\tau = \omega t$ and $\xi = kz$, the scheme of calculation of the amplitude values at the mesh points $(l\Delta\tau, j\Delta\xi)$ is as follows,

$$A_j^{l+1} = [-\mu^+ a_1 A_j^{l-1} + b_1 A_{j+1}^l + b_2 A_{j-1}^l + (\mu^+ f - g) A_j^l] / \mu^+ a_2, \quad (7)$$

$$B_j^{l+1} = [-\mu^- a_1 B_j^{l-1} + b_1 B_{j+1}^l + b_2 B_{j-1}^l + (\mu^- f - g) B_j^l] / \mu^- a_2, \quad (8)$$

where the auxiliary values are $a_1 = (n_j^{l-1})^2(1 - i\Delta\tau)$, $a_2 = (n_j^{l+1})^2(1 + i\Delta\tau)$, $b_1 = (\Delta\tau/\Delta\xi)^2(1 - i\Delta\xi)$, $b_2 = (\Delta\tau/\Delta\xi)^2(1 + i\Delta\xi)$, $f = (n_j^l)^2(2 + \Delta\tau^2)$, $g = 2(\Delta\tau/\Delta\xi)^2 + \Delta\tau^2$.

The stability of the algorithm is provided by the standard Courant condition between the step intervals of the mesh; in our notation it can be written as $\Delta\tau/\Delta\xi \leq n$. At the edges of the calculation region, we apply the so-called absorbing boundary conditions using the total field / scattered field (TF/SF) and the perfectly matched layer (PML) methods [24, 25].

As previously, we take the asymmetric structure consisting of 8 elementary units of two configurations of Section 3: with stronger ($m = 3$, $n = 5$) and weaker ($m = 5$, $n = 3$) radiation localization inside the defect. The permittivity of material in the nonlinear layers is described by Eq. (3) with the linear part $\bar{\varepsilon}_2 = 2$ and where $E_{in}(z) = E_{in}(t, z)$ is the actual value of the field. Since we describe the fields using dimensionless amplitudes $A(t, z)$ and $B(t, z)$, the normalized nonlinearity coefficient can be fixed to be $\bar{n}_2 = \bar{\varepsilon}_2/2\sqrt{\bar{\varepsilon}_2} = 0.001$. These parameters are close to the case considered in Section 3 for frequency-domain calculations. The incident radiation is assumed to be linearly polarized, so that the amplitudes on the boundary of the system are

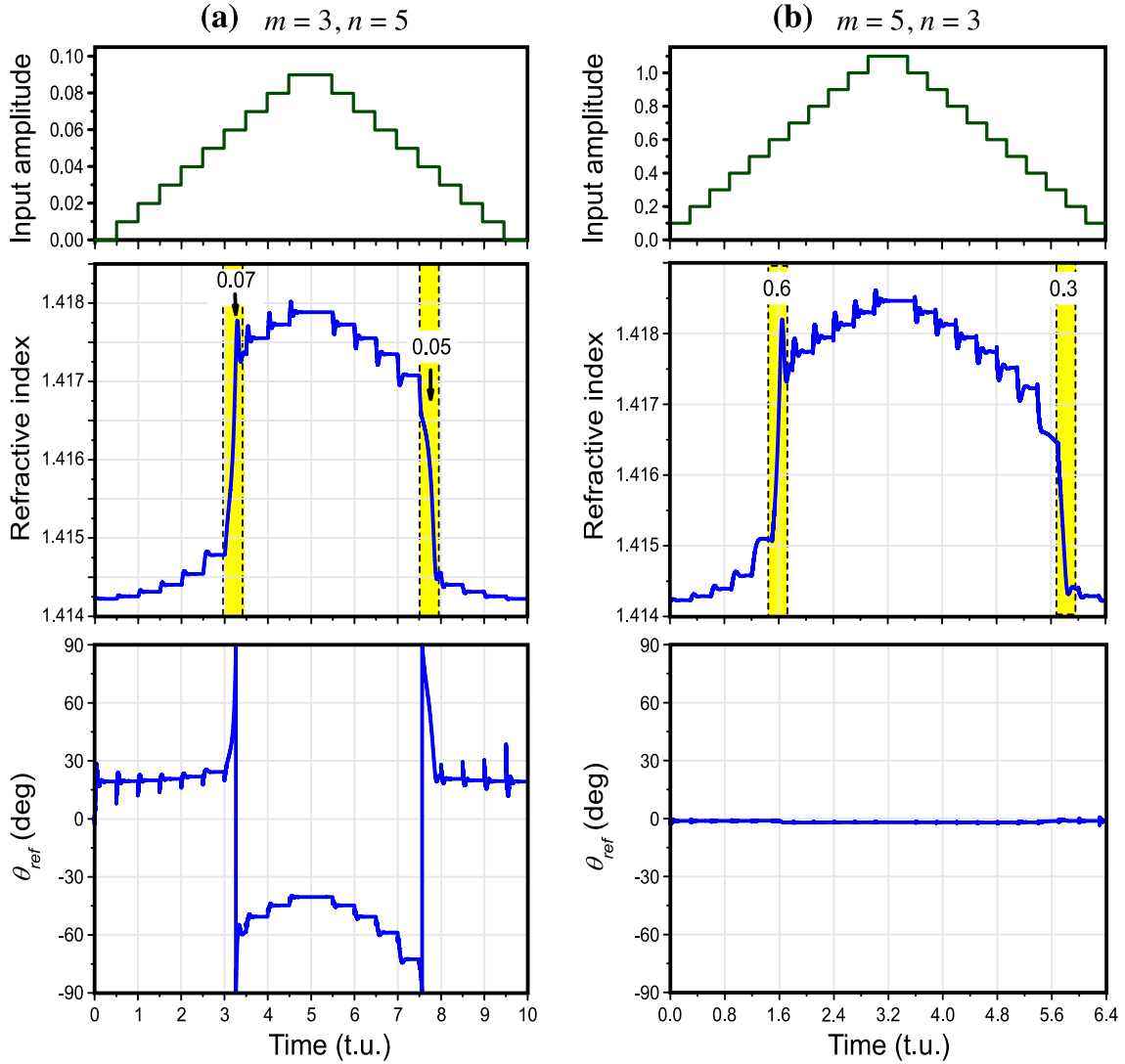


Figure 6. (Color online) The dynamics of the refractive index in the middle of the cavity layer and the polarization azimuth of reflected light for two configurations of asymmetric magnetophotonic crystal for (a) $m = 3, n = 5$ and (b) $m = 5, n = 3$. The time is given in the time units (t.u.) equal to $15000\lambda/c$, corresponding to 77.55 ps for the telecommunication wavelength of $1.55 \mu\text{m}$. The structure's parameters are as in Fig. 2.

equal, $A(t, 0) = B(t, 0)$. The normalized thickness of the layers is $D/\lambda = 0.183$.

To study the dynamics of polarization characteristics and achieve switching, we performed the calculations with incident light amplitudes gradually changing in a stepwise manner (Fig. 6). The time unit (t.u.) contains 15000 optical cycles, i.e. $1 \text{ t.u.} = 15000\lambda/c$. For the first configuration ($m = 3, n = 5$, see Fig. 6(a)), the incident amplitudes A and B were changed in the range 0.01–0.1 (first increasing and then decreasing) with the step 0.01; every amplitude was kept constant during 0.5 t.u. For the second configuration ($m = 5, n = 3$, Fig. 6(b)), the amplitudes were changed in the range 0.1–1.1 (the step is 0.1) after 0.3 t.u.

Figures 6(a) present clear evidence for the optical bistability in the structure with stronger light localization ($m = 3, n = 5$). The refractive index in the middle of the double layer (defect) and the polarization azimuth of reflected light undergo abrupt switching two times at different input radiation intensities. The corresponding amplitude values are 0.07 (when intensity is increasing) and 0.05 (when intensity is decreasing). The polarization azimuth at these points also switches by almost 90° , exhibiting an abrupt changes of sign.

The scenario turns out to be quite different in the weaker localization regime ($m = 5, n = 3$)

as seen in Fig. 6(b). Though the switching of the refractive index still does occur (albeit at amplitudes an order of magnitude higher – 0.6 and 0.3, respectively), the corresponding switching of the polarization state is negligible. One can conclude that the state of polarization remains almost unchanged: the polarization azimuth does not change its sign and stays near zero value.

The similarities and differences between the two configurations are highlighted in Fig. 7, which shows the explicit hysteresis loops obtained from the calculations in Fig. 6 by plotting the relevant characteristics (the refractive index inside the defect and the azimuth angle of the output polarization) at the quasi-steady state after each input intensity jump (after the transient oscillations have decayed) versus the input intensity. It is seen that even though the loops are quite narrow, they are undoubtedly present, confirming that polarization bistability investigated in Section 3 can actually be used for switching between almost orthogonal linear polarizations.

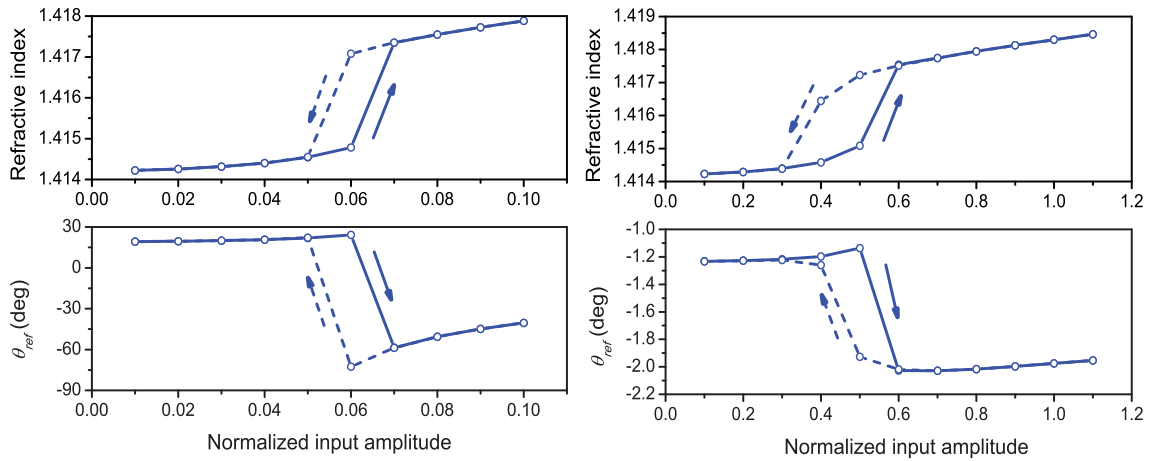


Figure 7. (Color online) The hysteresis loops for the refractive index in the middle of the cavity layer (n_2^{cavity}) and for the azimuth angle of reflected wave polarization (θ_{ref}) for the two configurations in Fig. 6.

5. Conclusions

In summary, we have investigated spectral and polarization properties of photonic multilayer structures combining both magneto-optic properties (the Faraday effect), nonlinear optical properties (the Kerr effect), and spatial inversion asymmetry. We have considered a periodic structure with an asymmetrically placed defect layer (a Fabry-Perot resonator with non-identical Bragg mirrors) as the example geometry, and performed both frequency-domain (nonlinear transfer-matrix) and time-domain (FDTD) calculations.

Even in the linear regime, we have demonstrated that an interplay of the Faraday effect and the spatial inversion asymmetry can give rise to significant enhancement of optical non-reciprocity, resulting in total 90° polarization rotation of reflected light [see Eq. (5)] for one direction of incidence only; for the opposite direction of incidence, polarization conversion effects were shown to vanish. This effect is explained by considering a different coupling strength between the cavity mode field and the incident field.

In the nonlinear regime, resonance bending and bistability in nonlinear reflection spectra has been demonstrated. In a properly designed multilayer (where output polarization is kept close to linear throughout the stop band of the Bragg mirrors), this bistability has been shown to result in bistability between distinct linear polarization states of the reflected output light.

Finally, our time-domain numerical simulations have confirmed that this polarization bistability can indeed be used for dynamic polarization switching, clearly exhibiting hysteresis phenomena (Fig. 7). Very strong dependence on the direction of incidence of the input light has been

demonstrated.

The results obtained can put forth new designs of both passive and active multilayer-based optical devices, such as polarization rotators, optical isolators, nonlinear polarization switches, and nonlinear optical diodes. Additionally, it has been found that there is a synergetic interplay between nonlinear, magneto-optical, and spatial inversion, giving rise to polarization properties not attainable otherwise. Investigating this interplay is a promising subject of further studies.

6. Acknowledgements

This work was supported by the Ukrainian State Foundation for Basic Research, project F54.1/004 and the Belarusian Foundation for Basic Research, project F13K-009. One of us (S.V.Z.) wishes to acknowledge partial financial support from the People Programme (Marie Curie Actions) of the European Unions 7th Framework Programme FP7-PEOPLE-2011-IIF under REA grant agreement No. 302009 (Project HyPHONE)

References

- [1] Landau, L.D.; Lifshitz, E.M. Electrodynamics of Continuous Media. In: *A Course of Theoretical Physics*; Vol. 8, Pergamon Press: Oxford, 1960.
- [2] Born, M.; Wolf, E. Principles of Optics. Pergamon Press: Oxford, 1970.
- [3] Lyubchanskii, I.L.; Dadoenkova, N.N.; Lyubchanskii, M.I.; Shapovalov, E.A.; et al. Magnetic photonic crystals. *Journal of Physics D: Applied Physics* **2003**, *36* (18), R277.
- [4] Inoue, M.; Fujikawa, R.; Baryshev, A.; Khanikaev, A.; Lim, P.B.; Uchida, H.; Aktsipetrov, O.; Fedyanin, A.; Murzina, T.; et al. Magnetophotonic crystals. *Journal of Physics D: Applied Physics* **2006**, *39* (8), R151.
- [5] Lu, Y.H.; Cho, M.H.; Kim, J.B.; Lee, G.J.; Lee, Y.P.; et al. Magneto-optical enhancement through gyrotropic gratings. *Opt. Express* **2008**, *16* (8) (Apr), 5378–5384.
- [6] Dokukin, M.E.; Baryshev, A.V.; Khanikaev, A.B.; et al. Reverse and enhanced magneto-optics of opal-garnet heterostructures. *Opt. Express* **2009**, *17* (11) (May), 9062–9070.
- [7] Novitsky, D.V. Asymmetric light transmission through a photonic crystal with relaxing Kerr nonlinearity. *Europhys. Lett.* **2012**, *99* (4), 44001.
- [8] Novitsky, D.V. Controlled absorption and all-optical diode action due to collisions of self-induced-transparency solitons. *Phys. Rev. A* **2012**, *85* (Apr), 043813.
- [9] Miroshnichenko, A.E.; Brasselet, E.; Kivshar, Y.S. Reversible optical nonreciprocity in periodic structures with liquid crystals. *Appl. Phys. Lett.* **2010**, *96* (6), 063302–063302–3.
- [10] Grigoriev, V.; Biancalana, F. Bistability, multistability and non-reciprocal light propagation in Thue–Morse multilayered structures. *New Journal of Physics* **2010**, *12* (5), 053041.
- [11] Grigoriev, V.; Biancalana, F. Bistability and stationary gap solitons in quasiperiodic photonic crystals based on Thue–Morse sequence. *Photonics and Nanostructures - Fundamentals and Applications* **2010**, *8* (4), 285 – 290. Tacona Photonics 2009.
- [12] Tuz, V.R.; Prosvirnin, S.L. Bistability, multistability, and nonreciprocity in a chiral photonic bandgap structure with nonlinear defect. *J. Opt. Soc. Am. B* **2011**, *28* (5) (May), 1002–1008.
- [13] Tuz, V.R.; Prosvirnin, S.L.; Zhukovsky, S.V. Polarization switching and nonreciprocity in symmetric and asymmetric magnetophotonic multilayers with nonlinear defect. *Phys. Rev. A* **2012**, *85* (Apr), 043822.
- [14] Zvezdin, A.K.; Kotov, V.A. Modern Magneto-optics and Magneto-optical Materials. Institute of Physics Publishing: Bristol and Philadelphia, 1997.
- [15] Palik, E.D. Handbook of Optical Constants of Solids. Academic Press: Boston, 1991.
- [16] Tuz, V.; Vidil, M.; Prosvirnin, S. Polarization transformations by a magneto-photonic layered structure in vicinity of ferromagnetic resonance. *J. Opt.* **2010**, *12*, 095102.
- [17] Jonsson, F.; Flytzanis, C. Optical amplitude and phase evolution in nonlinear magneto-optical Bragg gratings. *J. Nonlinear Opt. Phys. Mat.* **2004**, *13* (1), 129–154.
- [18] Jonsson, F.; Flytzanis, C. Nonlinear Magneto-Optical Bragg Gratings. *Phys. Rev. Lett.* **2006**, *96* (Feb), 063902.
- [19] Zheludev, N.I. Polarization instability and multistability in nonlinear optics. *Sov. Phys. Usp.* **1989**, *32*, 357–375.
- [20] Zhukovsky, S.V.; Smirnov, A.G. All-optical diode action in asymmetric nonlinear photonic multilayers with perfect transmission resonances. *Phys. Rev. A* **2011**, *83* (2) (February), 023818.
- [21] Zhukovsky, S.V. Perfect transmission and highly asymmetric light localization in photonic multilayers. *Phys. Rev. A* **2010**, *81* (5) (May), 053808.
- [22] Wang, R.; Dong, J.; Xing, D.Y. Defect studies in a one-dimensional photonic band gap structure. *Physica Status Solidi (b)* **1997**, *200* (2), 529–534.
- [23] Novitsky, D.V. Pulse trapping inside a one-dimensional photonic crystal with relaxing cubic nonlinearity. *Phys. Rev. A* **2010**, *81* (May), 053814.
- [24] Taflov, A. Computational electrodynamics: The finite-difference time-domain method. Artech House: Boston, 1995.
- [25] Anantha, V.; Taflov, A. Efficient modeling of infinite scatterers using a generalized total-field/scattered-field FDTD boundary partially embedded within PML. *IEEE Trans. Antennas Propag.* **2002**, *50*, 1337–1349.